JET-P(95)33

Recent Results of ICRF Heating on JET

D F H Start, G Bell[1], V P Bhatnagar, M Bures, G A Cottrell, L-G Eriksson, B Fechner, R Goulding[1], C Gormezano, A Howman, J Jacquinot, A Kaye, P Lamalle, F Nguyen[2], E Righi, F Rimini, A Sibley, A C C Sips, B J Tubbing, T Wade, D Ward.

JET Joint Undertaking, Abingdon, Oxfordshire, OX14 3EA, UK.
[1] Oak Ridge National Laboratory, Oak Ridge, Tennessee, USA.
[2] CEA Cadarache, France.

Preprint of a paper to be submitted for publication in
the proceedings of the 11th Topical Conference on RF Power into Plasmas,
Palm Springs, USA.

ABSTRACT

During ICRF heating experiments, the new four–strap A2 antennas on JET have coupled 16.5MW of power into single null divertor plasmas (fig 1). In combined heating experiments a maximum of 32MW has been achieved by adding 15MW of hydrogen minority ICRH to 17MW of neutral beam injection (NBI). This combined heating power is a record for the present campaign and was achieved in a high density, strongly radiating, reactor–like scenario with 'grassy' ELMs. Central electron temperatures close to 15keV have been obtained with both RF–only and combined heating in ELM–free plasmas which were created with high flux expansion in the divertor region and which were substantially triangular ($\delta \simeq 0.3$). Similar discharges were used to obtain the highest D–D reactivity in JET with NBI. The addition of hydrogen minority ICRH to these plasmas increases both the reactivity and the H–factor obtained by comparing the thermal energy content to the ITERH93–P scaling. RF–only H–modes have been produced in plasmas with currents (I_p) up to 4.7MA and the power thresholds are similar those with NBI. At I_p = 4.7MA and a toroidal field (B_t) of 3.2T, a plasma energy content of 7MJ was achieved with 8MW of 51.3MHz ICRH in $0\pi0\pi$ phasing. The heating efficiency, as determined from power modulation experiments, is close to 100% with $0\pi0\pi$ and $0\pi\pi0$ phasing. The efficiency decreases for phasings such as $00\pi\pi$ and monopole which produce average values of the parallel wavevector less than 3.5m^{-1}. However, the recent introduction of a separator limiter at the centre of one antenna has improved its heating efficiency for perpendicularly launched waves and such separators will be fitted to all antennas in the near future.

1. INTRODUCTION

The ion cyclotron resonance heating system on JET has been modified extensively to operate with the new divertor configurations. Each of the four antennas has four coherently excited current straps which can produce a wide range of radiation patterns by varying the relative phasing between currents. For heating purposes the characteristics of 0000, $00\pi\pi$, $0\pi\pi0$ and $0\pi0\pi$ phasings have been studied extensively which give parallel wavevectors between zero and 8m^{-1}; travelling waves for current drive applications have also been launched using 60^0 and 90^0 phasings. The control system has been upgraded and a new set of electronics has been installed to operate the

matching of four straps simultaneously. As on the previous system, automatic matching is accomplished by feedback on frequency, stubs, trombones and plasma position. An example is shown in fig 2. At the

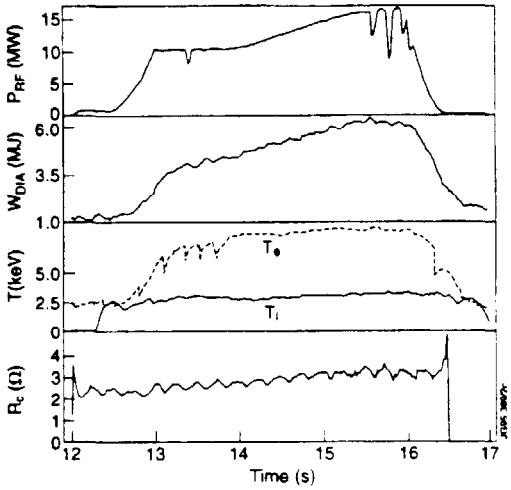

Fig 1 16.5MW of ICRH and a 2.5s Monster sawtooth

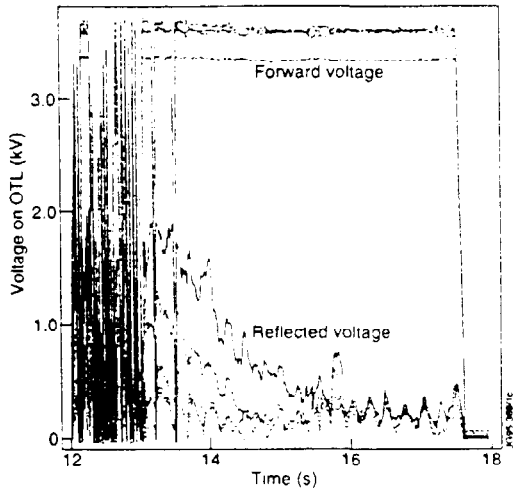

Fig 2 Automatic matching of four antenna straps

beginning of the RF pulse the reflection coefficient exceeds the trip level. After 1sec the tuning elements have moved to remove most of the trips and the reflected power is then quickly reduced to almost zero. The system is also fitted with decouplers between the outerstraps of three antennas. These decouplers are specific to current drive operation and their purpose is to compensate for the inductive coupling of power between the antenna straps, particularly with 90^0 phasing in low coupling scenarios. Presently, this feature is being commissioned.

This paper reviews the experience and results gained with the new system in a wide variety of magnetic configurations and plasma conditions. In the next section we describe the electrical characteristics of the antennas, their behaviour in coupling to plasma and a new method of determining the scattering matrix on a single plasma pulse. In section 3 we present results obtained with high power in radiative divertor plasmas and investigate the efficacy of using centrally peaked RF heating profiles compared with the flat NBI profiles produced at densities around $6x10^{19}m^{-3}$. Section 4 describes the attainment of 15keV central electron temperature and enhanced H–factors with RF in high flux expansion divertor plasmas which are the best candidates for the JET D–T phase. The power threshold for RF–only H–modes is shown to be similar to that for NBI in section 5 and section 6 discusses the heating efficiency for various antenna phasings.

2. CHARACTERISTICS OF THE A2 ANTENNAS

Extensive coupling studies have been carried out for the phasings mentioned in section 1 and for frequencies of 32MHz, 43MHz, 48MHz and 52MHz. At a given frequency, the coupling resistance, R_c, averaged over current straps, increases as the parallel wavevector (k_z) decreases. The resistance R_c is defined as the characteristic impedance of the feed lines (30Ω) divided by the

voltage standing wave ratio on these lines. For monopole phasing (k_z = $0m^{-1}$), $<R_c>$ is typically 5Ω and decreases to 2Ω for dipole ($0\pi0\pi$) phasing with k_z = $8m^{-1}$. At a given frequency and phasing, the values of R_c are generally different for different straps. In part, this is expected due to the inductive coupling between straps combined with the fact that the inner straps have two nearest neighbours whereas the outer straps have only one. However, the observed asymmetry is much larger than predicted for most of the operating space. An example is shown in fig 3 where the ratio of the coupling resistance for the inner and outer straps is plotted against frequency for dipole phasing.

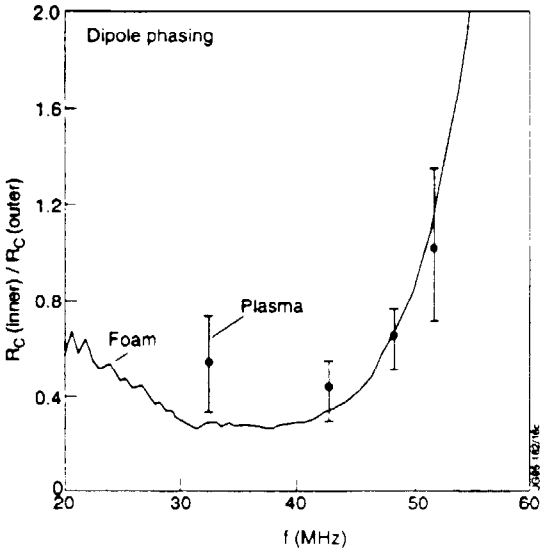

Fig 3 Coupling resistance ratios for inner and outer straps

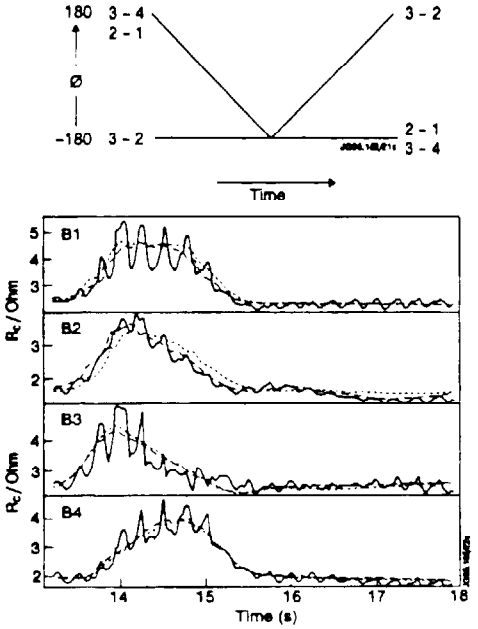

Fig 4 Scattering matrix evaluation using phase ramps

The points are measurements on plasma and the solid curve is a measurement on the prototype antenna with foam loading. At 52MHz there is little asymmetry but below this frequency the coupling resistance of the inner straps can be as small as one third of that of the outer strap. Above 52MHz the inner straps couple better than the outer straps. Scattering matrix measurements on the prototype antenna show that the major cause of the coupling imbalance is the high impedance of the crossover links ($Z_0 \simeq 70\Omega$) which connect the inner straps to the 30Ω feed lines. Adding capacitance to the crossover link to convert it to a 30Ω line reduces the imbalance but does not eliminate it completely; there appears to be a residual loading dissimilarity between the inner and outer straps.

The measurement of scattering matrices of the antenna has proved to be a powerful investigative tool. Recently a technique has been developed to measure the matrix with plasma loading in a single RF pulse[1]. The method uses a phase ramp over a period of a few seconds which is slow enough to allow the system to maintain a good match. The scattering matrix is then derived by fitting the time evolution of the forward and reflected voltages on the feed lines. A typical phase ramp is shown in fig 4 which varies the phase

difference between the outer and adjacent inner straps (e.g. 1 and 2) during the first half of the pulse while maintaining a constant 180^0 phase diffferncе between the inner straps (2 and 3). In the second part of the pulse the ramp is applied to the inner straps while each outer strap maintains a 180^0 phase relative to its neighbouring inner. As the phase is ramped the strength of the R_c variation reflects the amplitude of the inter–strap coupling terms (fig 4). In this case at 51MHz the variation of R_c in the first part of the pulse is due to the coupling between the inner and outer straps. The small variation in the second part is due to a cancellation between the inner–inner and outer–inner couplings.

3. HIGH DENSITY RADIATIVE DIVERTOR DISCHARGES

The maximum conbined RF and NBI power of 32MW has been injected into a 2.5MA, 3.4T single null X–point deuterium plasma. The NBI was injected earlier than the RF to establish an H–mode with 'grassy' ELMs for good RF coupling ($<R_c> = 3\Omega$). The density was increased during the beam–only phase to a central value $n_e(0) = 6.4x10^{19}m^{-3}$. The ICRH was hydrogen minority heating with $0\pi\pi0$ phasing at 51.3MHz which gave on–axis power deposition. Nitrogen was injected to produce impurity seeding such that 60% of the input power was radiated in the divertor region. The evolution of the plasma parameters is shown in fig 5.

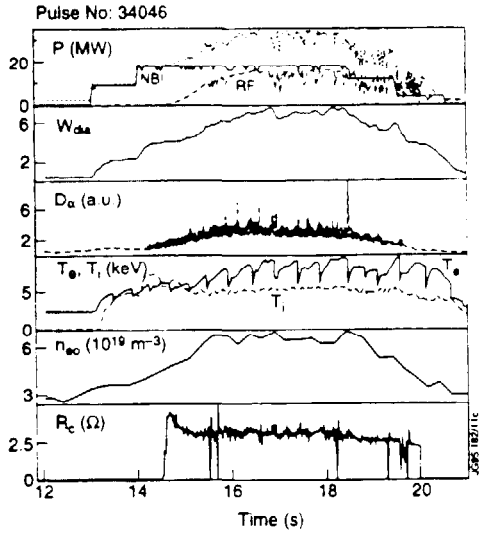

Fig 5 32MW of combined ICRH and NBI in a radiative divertor plasma.

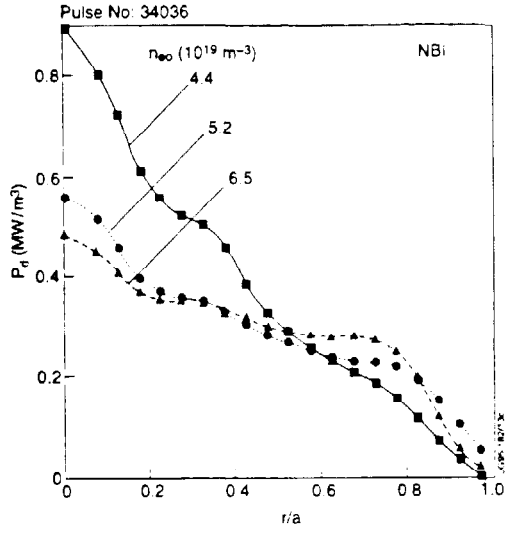

Fig 6 NBI power deposition profiles as density increases

At a density of $6.4x10^{19}m^{-1}$ the power density profiles of the neutral beam injection and ICRH are quite different with the former being rather flat in minor radius as shown in fig 6. The fast wave has no accessibility problems at high density and so produces a peaked profile (fig 7). The question arises as to whether such peaked profiles enhance the global confinement since the power is placed in a region of low thermal conductivity. To investigate this point we have plotted in fig 8 the H–factors based on ITER89–P and

ITERH93–P scaling laws. These are, respectively, given by

$$\tau_{89} = 0.048\ I^{0.85}\ (n/10)^{0.1}\ B^{0.2}\ P^{-0.5}\ R^{1.5}\ \epsilon^{0.3}\ \kappa^{0.5}\ M^{0.5} \qquad (1)$$

and

$$\tau_{93} = 0.036\ I^{1.08}\ n^{0.17}\ B^{0.32}\ P^{-0.67}\ R^{1.79}\ \epsilon^{-0.11}\ \kappa^{0.66}\ M^{0.41} \qquad (2)$$

where I(MA) is the plasma current, n($10^{19}m^{-3}$) is the density, B(T) is the toroidal field P(MW) is the loss power, R(m) is the major radius, ϵ is the inverse aspect ratio, κ is the elongation and M is the ion atomic number.

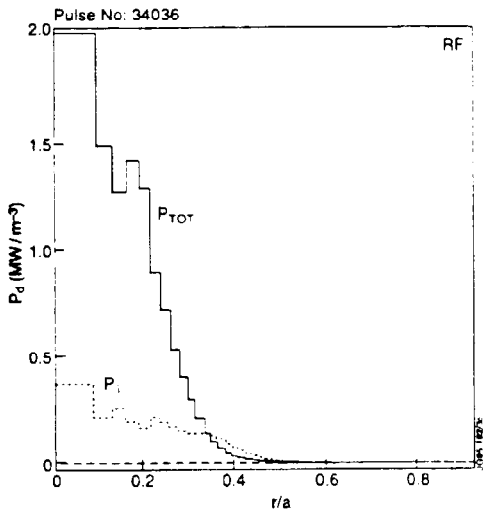

Fig 7 ICRH power density profile

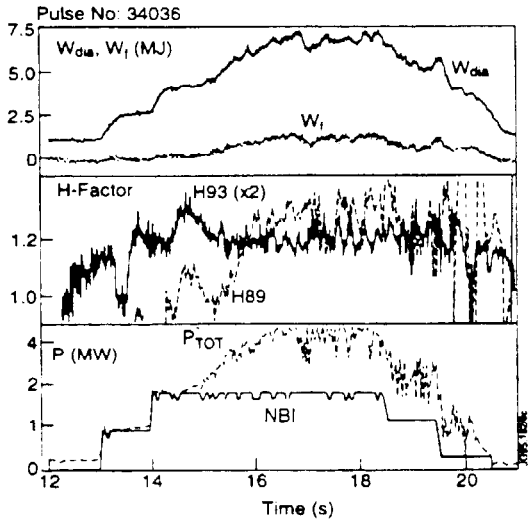

Fig 8 H–factor for ITER89–P and ITERH93–P

Both comparisons are made because of the complication introduced by a significant fast ion population: ITER89–P scaling was derived without fast ion energy (W_f) subtraction, whereas ITERH93–P is based on thermal energy content only. Note that in general these radiative divertor plasmas are relatively poor H–modes with confinement times only 1.3 times L–mode. At 15sec into the discharge the energy content has reached steady state with 17MW of NBI and the H–Factor(89–P) is unity. As the RF power is applied this factor increases to 1.3 and so on this basis there is an enhancement of the H–factor. However in the case of ITERH93–P, where only thermal energy used, there is no corresponding increase. In other discharges there is a small increase in the ITERH93–P H–factor but it is always less than 5%.
This result is somewhat surprising and so to estimate what level of increase should be expected a heat transport simulation of discharge 34036 has been carried out. We assume that the power scaling of the confinement time is due to a temperature dependence of the thermal conductivity. The scaling of τ with power in equations 1 and 2 then imply $\chi\ \alpha\ T$ for ITER89–P and $\chi\ \alpha\ T^2$ for ITERH93–P. To take account of χ varying with T, the steady state heat diffusion equation

$$\frac{1}{r}\frac{\partial}{\partial r}\left(rn\chi\frac{\partial T}{\partial r}\right) + P_d(r) = 0 \qquad (3)$$

is solved iteratively. First an initial $\chi(r)$ profile is chosen which reproduces the profile of the average temperature, $(T_e + T_i)/2$, for the NBI only case at 15sec when the density has reached $6x10^{19}m^{-3}$ and the energy content is in

steady state. This $\chi(r)$ profile is then used with the NBI + ICRH power density profile to calculate an initial T(r) profile for the combined heating at the same density. The conductivity is then renormalised at each radius according to which temperature scaling is being investigated and equation (3) is solved again to obtain a new temperature profile. This process is repeated until the value of the central temperature converges. The thermal energy content and the H–factor are then calculated. For discharge 34036 we find that the ITERH93–P scaling predicts an H–factor increase of about 20%. Thus we are attempting to observe a modest increase and the discrepancy between this value and the maximum observed (5%) can be strongly affected, for example, by inacuracies in subtracting the fast ion energy content or by changes in the level of radiated power from the plasma core. These uncertainties will be minimised as the data are more carefully validated.

4. HIGH FLUX EXPANSION PLASMAS

The longest ELM–free H–modes and highest D–D reaction rates in JET are obtained in configurations with substantial triangularity ($\delta \simeq 0.3$) and strongly expanded flux surfaces in the divertor. Such discharges are leading candidates for the next tritium phase on JET. In this section we present results of RF heating in this type of plasma with I_p = 3MA, and B_t = 3.1T.

4.1 Central Electron Temperatures with ICRH and Combined Heating

In the ICRH– only case 10MW of hydrogen minority heating was applied initially to form an ELMy H mode at a density of $3.5 \times 10^{19} m^{-3}$. The power was the reduced to 7MW, and the density to $2.5 \times 10^{19} m^{-3}$. The central electron temperature $T_e(0)$ was well above 10keV for the whole RF pulse and reached a record value of 14.5keV during the low density phase. The $T_e(r)$ profile at this point is shown in fig 9. The fast hydrogen ion energy content reached 2MJ which is reproduced by PION code calculations. The slowing down time under these conditions was about 4s in the centre of the plasma. Figure 9 also shows the electron and ion temperature profiles obtained with a combination of 4MW of ICRH and 4MW of NBI in a configuration which was almost a double null X–point.

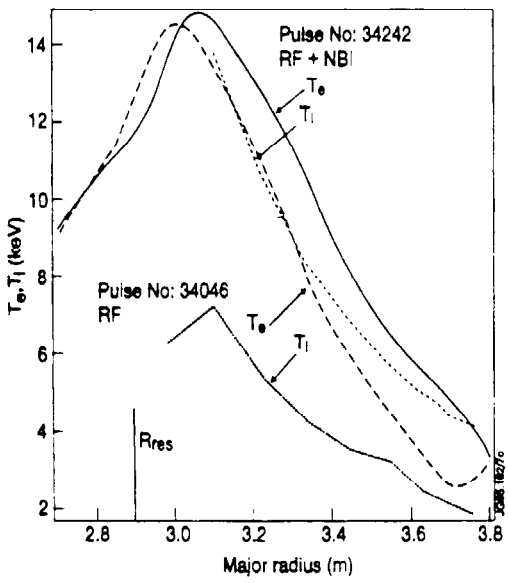

Fig 9 T_e and T_i profiles

In this case $T_e(0)$ is 15keV and $T_i(0)$ is 14keV. The highest values of $T_e(0)$ were achieved with the resonance about 0.2m on the high field side of the plasma centre which is where the fast wave is focussed.

4.2 H–Factor Enhancement with ICRH.

The addition of on–axis ICRH to ELM–free H–modes created by NBI can enhance the performance of these plasmas as shown in fig 10 which compares

a case of combined heating (34454) with a pulse with NBI alone (34443). Both plasmas have LHCD to drive off–axis current and maintain q(0) > 1, with no sawteeth, prior to the beam input. Note the increases in reactivity (R_{dd}) and energy content for the combined heating case. Initial TRANSP calculations show that the increased reactivity is due to increased ion pressure and does not require second harmonic beam acceleration for interpretation. The increased energy content is partly due to the higher power, partly to the fast ion contribution and partly to a 20% enhancement of the thermal H–factor derived from ITERH93–P scaling as shown in fig 11.

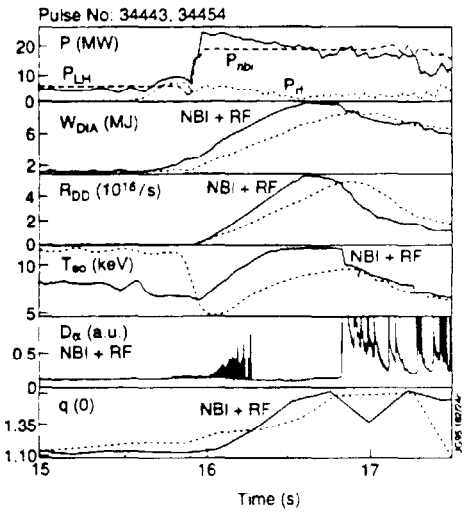

Fig 10 Enhanced ELM–free plasmas with NBI+ICRH

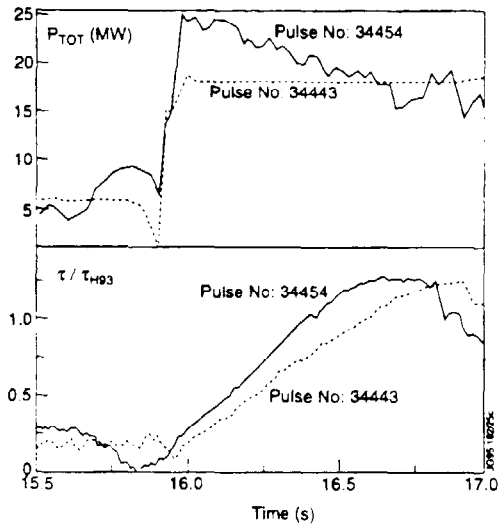

Fig 11 H–factors for the discharges in fig 10

5. H–MODES WITH ICRH ALONE.

There have been extensive studies of the H–mode power threshold in JET, particularly its scaling with plasma density which is of interest to ITER. Data have been obtained for both ICRF and NBI for plasma currents in the range 1MA to 4.7MA. The results are shown in fig 12 where the total input power to produce the H–mode is plotted against the product of average density and toroidal field. The RF data are for dipole and $0\pi\pi0$ phasings. The power threshold for RF is generally similar to that for NBI except for Be divertor tiles where it is significantly less. The scaling appears to be in good agreement with the ASDEX/DIID scaling, namely

$$P_{tot}/S = 0.0044 n_e B_t$$

where S is the surface area of the plasma in m^2, P is in MW, n_e is in $10^{19} m^{-3}$ and B_t is in tesla.

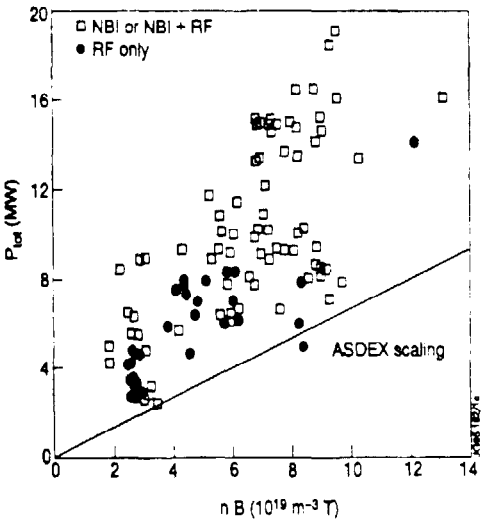

Fig 12 H–mode threshold

6. HEATING EFFICIENCY

The heating efficiency of the A2 antennas has been measured using power modulation. The power reaching the central good confinement region is deduced from the modulation of the energy content and is compared to the input power to obtain the efficiency. Experiments were carried out for both heating and current drive phasings. Three antennas were set to dipole phasing to ensure sufficient fast ion energy for good damping. The fourth antenna was operated with the phasing under study. The hydrogen minority resonance was placed at the plasma centre. For dipole and $0\pi\pi0$ phasing the efficiency is close to 100%. However, for values of the wavevector less than $4m^{-1}$ the efficiency is reduced as wave is launched ever more perpendicular to the magnetic field. For monopole phasing, practically no heating was observed. The phasings which produced low heating also generated hot spots on the poloidal limiters near the antennas. The hot spots disappeared when the magnetic field was aligned with the antenna screen bars suggesting that the effect was connected with RF sheath rectification. Such effects are expected to be more severe in the A2 antennas compared with the A1 antennas since the present four strap system has three times the toroidal extent of the two strap design. A remedy is to install a 'separator' limiter at the centre of the antenna. A prototype has been successfully tested although arcing problems limited the results for monopole and $00\pi\pi$ phasings. Modified separators will be fitted to all antennas in the present shutdown.

7. SUMMARY

The new ICRF heating on JET routinely operates above 10MW and has coupled a maximum power of 16.5MW. A reduced coupling has been found for the inner straps below 50MHz and it is due to an impedance transformation generated by the crossover current feeds. In the present shutdown it is planned to modify the antennas to ameliorate the coupling imbalance and also to install separators on all antennas to improve the heating for the phasings which give good coupling. Combined heating with ICRH and NBI has achieved 32MW into radiative divertor plasmas and a small improvement in performance due to the central power deposition by the ICRF has been seen. However, a more substantial enhancement of the H–factor have been produced by adding RF to NBI in ELM–free, high flux expansion plasmas which will probably be the type of discharge used in the next D–T experiments. Central electron temperatures close to 15keV have been achieved in these plasmas both with ICRH alone and with combined heating. Changes to the system to improve its resilience to ELMs are being investigated and some success has been achieved by installing a faster re–application of power after ELM–induced trips. A more radical system[2]. using prematched stubs and fast frequency tuning to maintain the match during an ELM, is under study.

REFERENCES

1) P U Lamalle et al., Proceedings of the 22nd EPS Conference on Controlled Fusion and Plasma Physics, to be published.
2) J Jacquinot, private communication.